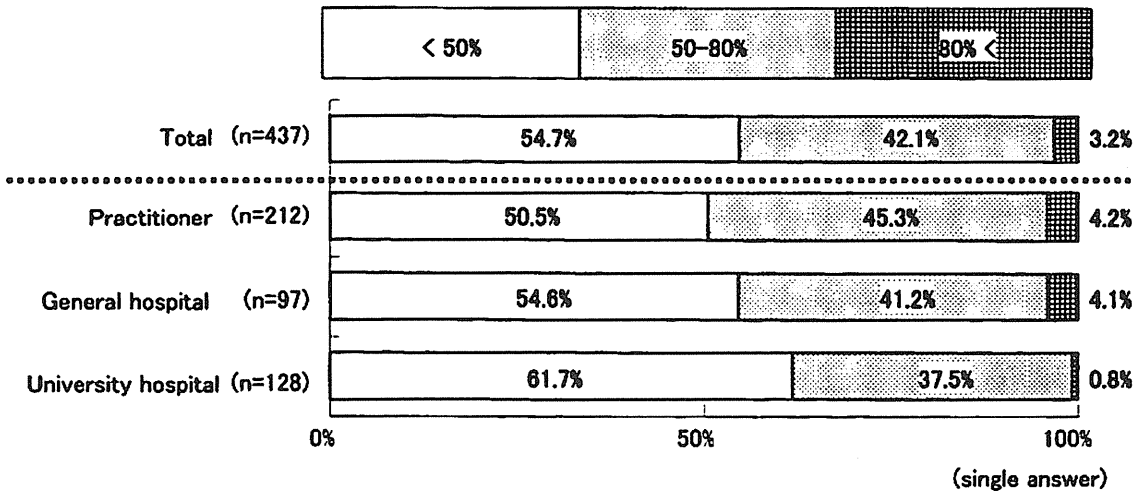

Fig. 6 : The identification rates of the causative allergens for contact dermatitis with Japanese standard allergens.
* Question for doctors answered "Regularly performed" and "Sometimes performed"about the frequency of patch testing.

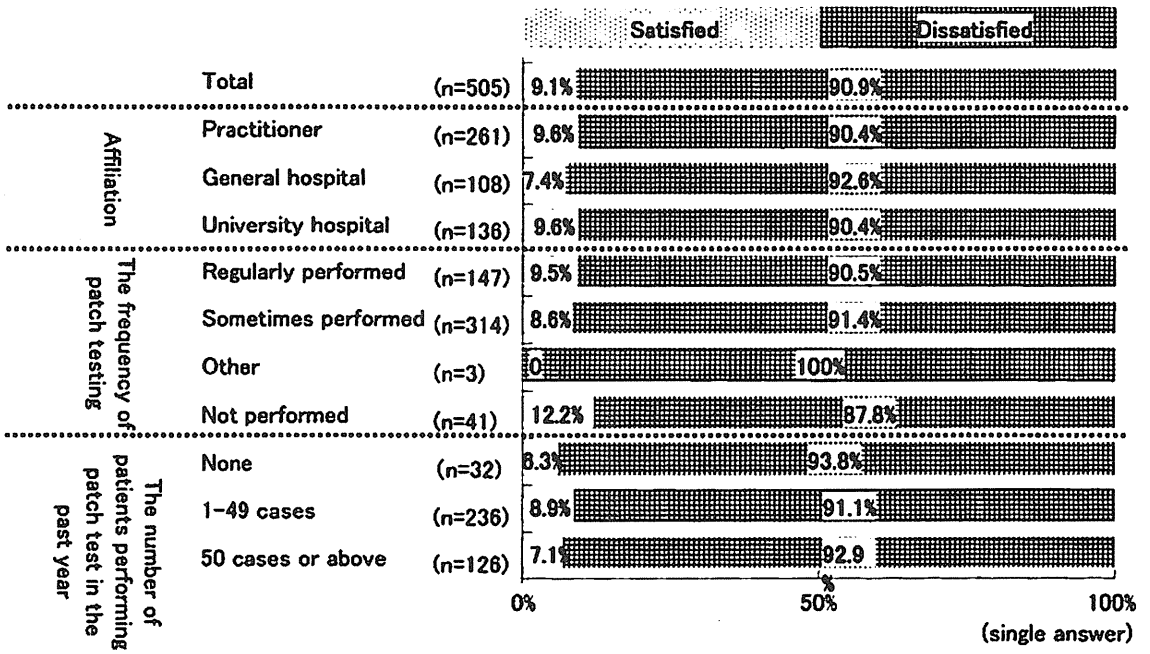

Fig. 7 : The degrees of satisfaction with patch test allergens marketed in Japan.

ストの準備に要する人件費などを勘案すると，パッチテストをすると赤字となる。そして貼付数が多ければ赤字額は増える一方である。このような現状を踏まえ，パッチテストの保険適応における問題の有無を調査したところ，83.6%（418名）が問題があると答え，その問題点としては，保険点数の低さのためが最も多い結果であった（Fig. 9)。さらに，適切だと考える保険点数については，1ヵ所あたり30点という回答が最も多い結果であった（Fig. 10)。自由記載欄には，現在の1ヵ所あたりの保険点数とは別に判断料や基本料などを算定するという意見もあった。

6．TRUE Testの認知と必要性について

2010年5月に保険適応となったready-to-useのTRUE Test[2,3]（日本での商品名：パッチテストテープ）については回答の約半数（52.4%）がその存在を知らないという結果であり，知っているが使用したことはないという回答は46.0%で，全体の

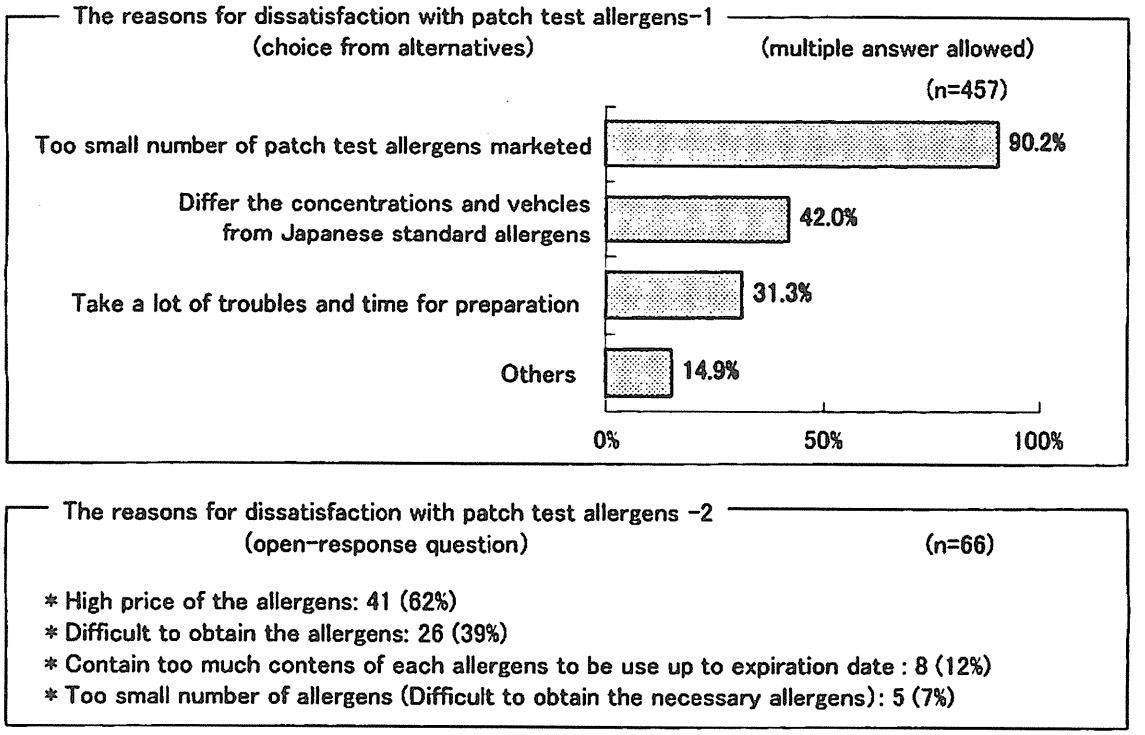

Fig. 8 : The reasons for dissatisfaction with patch test allergens marketed in Japan.

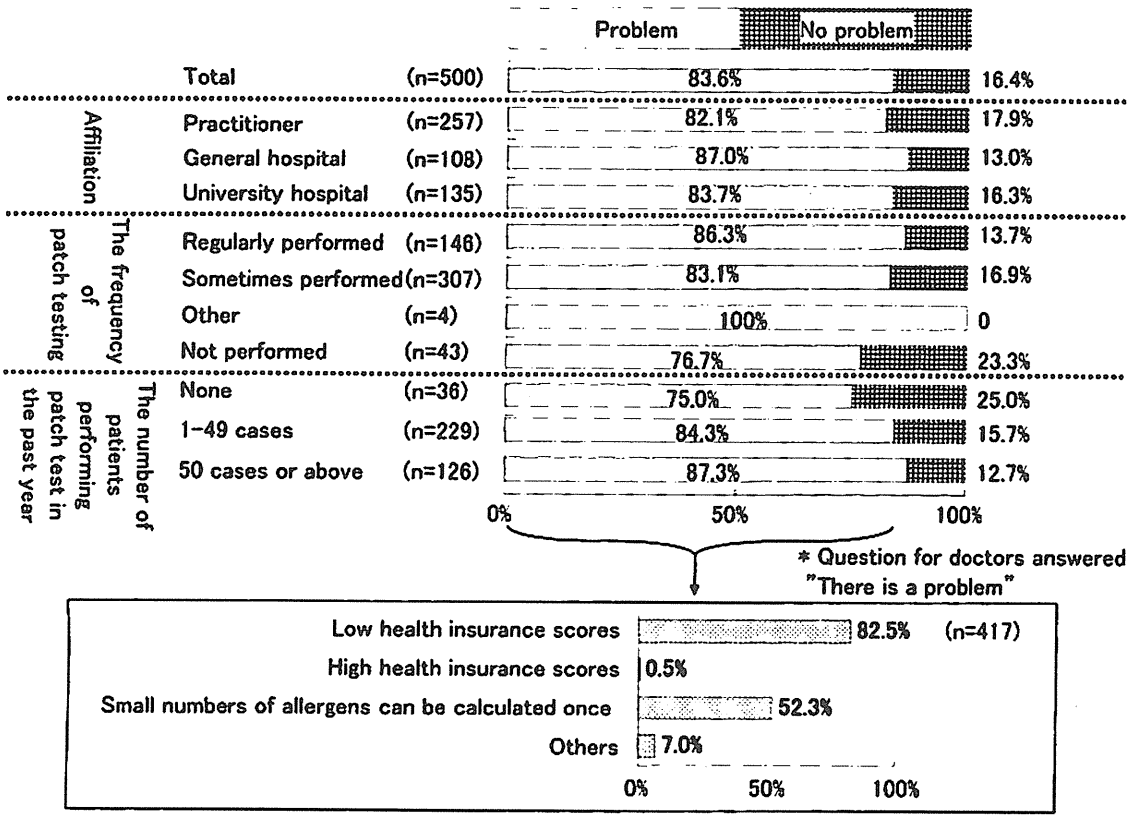

Fig. 9 : The health insurance problems in patch testing.

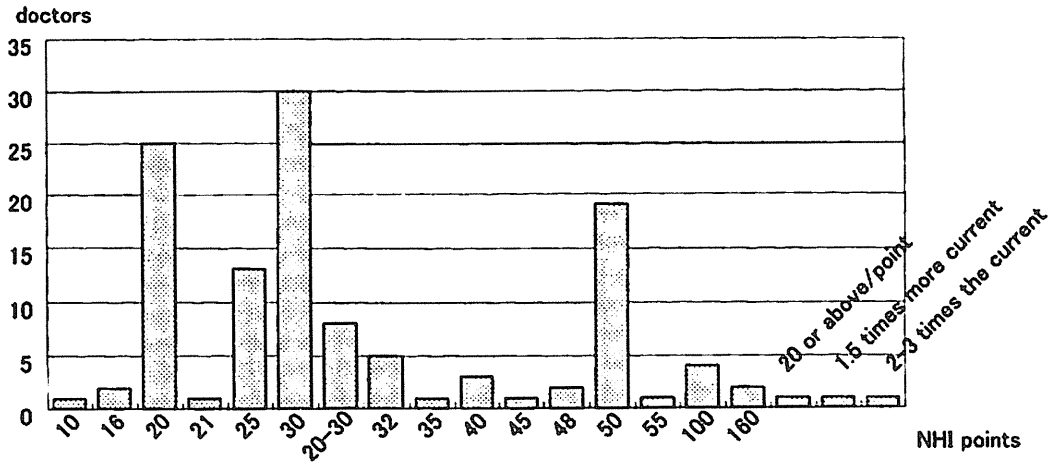

Other opinions

* 30/point, 1,000/points more than 22
* 30/point, 750/points more than 22
* 30/point, more than 500/series
* 50/point, have upper limit
* 50/point (1-10points), 35/points (more than 11), Upper limit is 1,000
* 160/series (less than 21 points)
* 200/series
* 400/series
* 500/series
* 200/series (less than 21 points), 500/series (22 points or above)
* 350/series (less than 20 points), 500/series (more than 20 points), 700/series (more than 30 points)
* 700/series (more than 22 points)
* 700/series
* 1,000/series
* 3,500 (more than 50 points)
* 150 (determine fee) and 100/point
* 300 (base fee) and 16/point
* 200 (base fee) and reagent cost

Fig. 10：The patch test health insurance score considered appropriate.

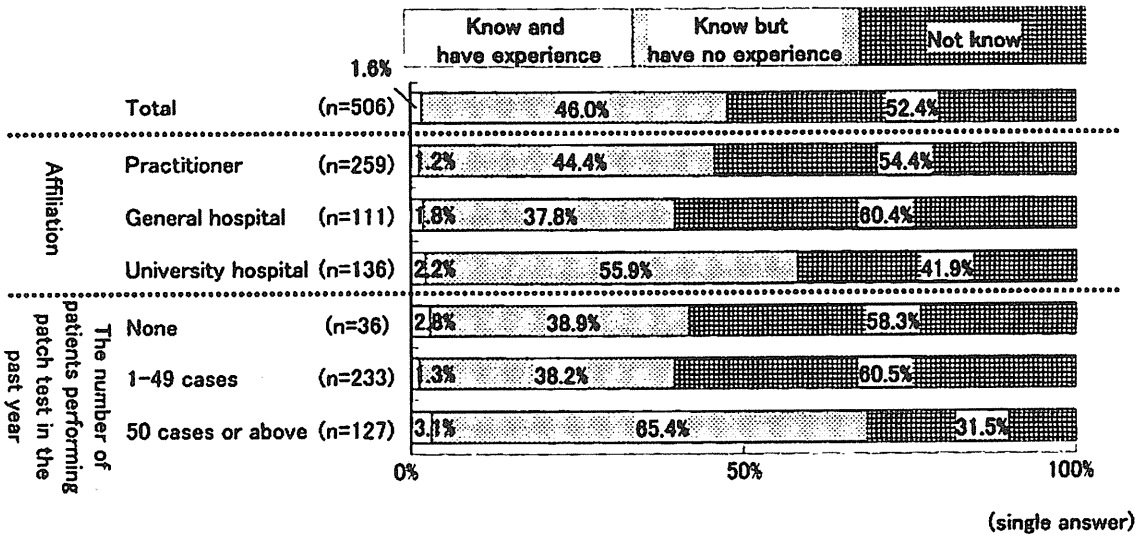

Fig. 11：The awareness and usage of the TRUE Test.

98.4%は使用経験がない結果であった（Fig. 11）。しかしながら，TRUE Testを84%が必要と感じており，TRUE Testの販売によりわが国でのパッチテスト使用症例は増えると感じているのはその81.8%であった（Fig. 12）。TRUE Testを不要と考える回答は77名（16.0%）あったがその理由としては必要なアレルゲンのみでよいというものであった（Fig. 13）。

考　案

日本皮膚科学会接触皮膚炎診療ガイドライン[9]では，パッチテストは接触皮膚炎の原因検索を行う際

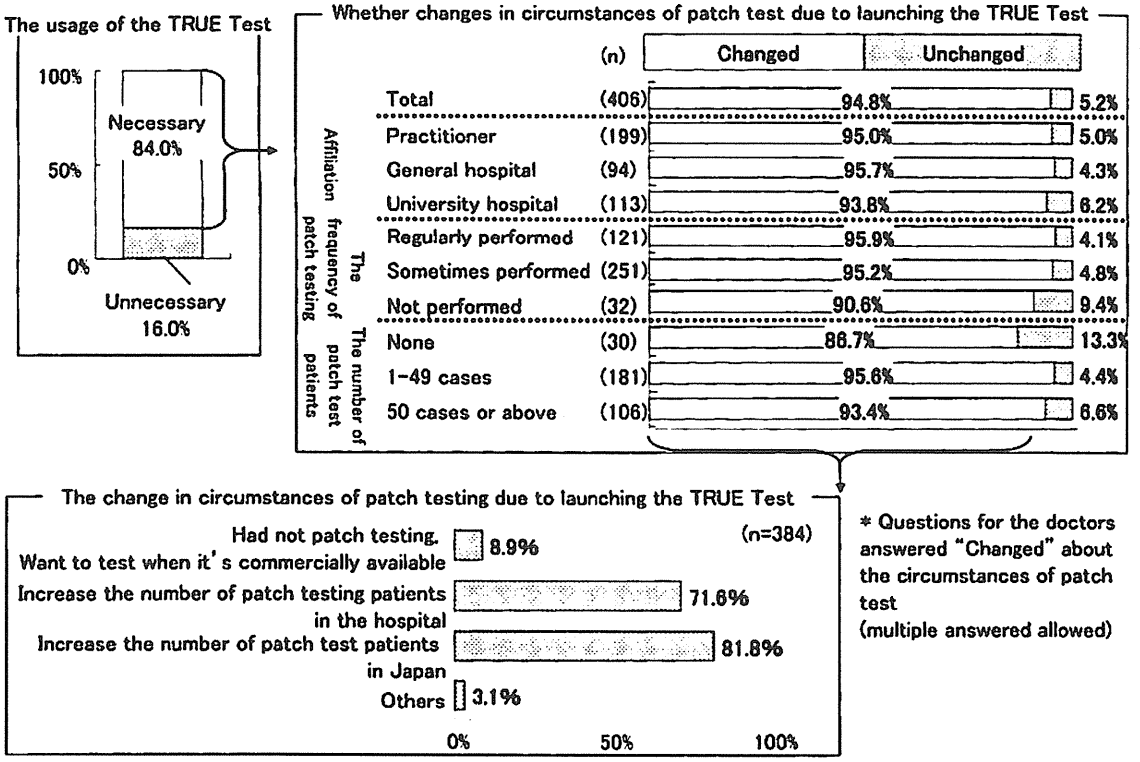

Fig. 12 : Expected in circumstances of patch test after launching of the TRUE Test.

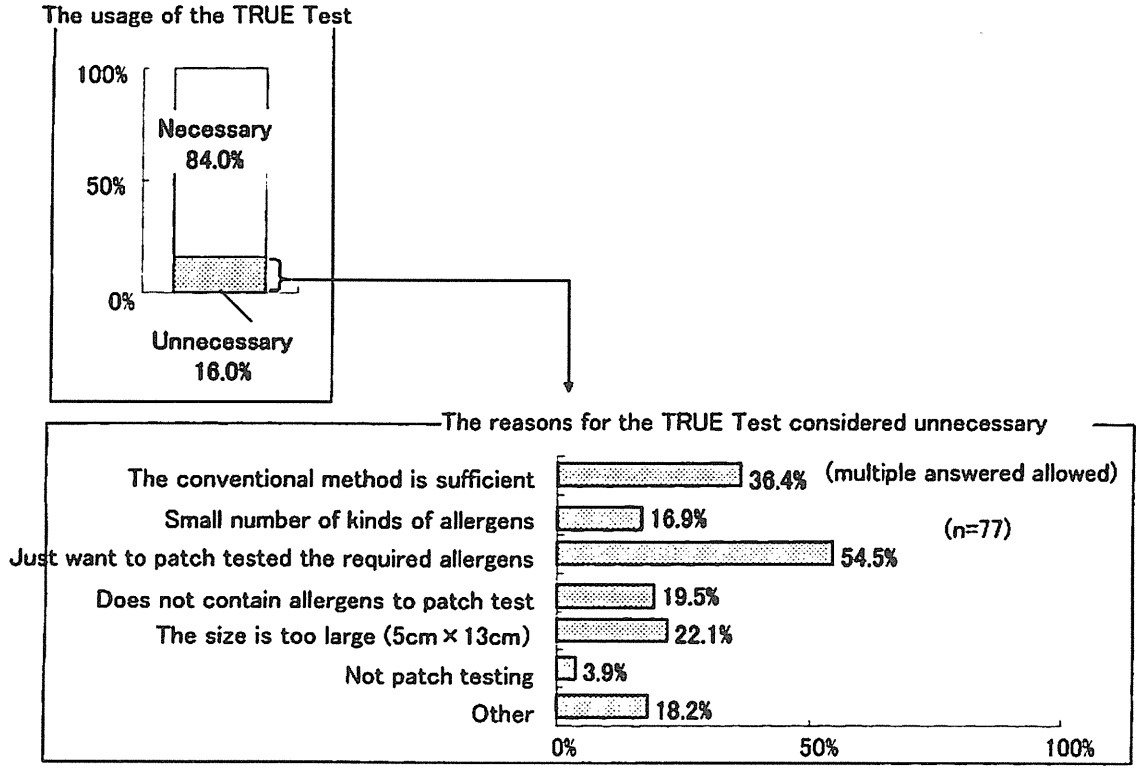

Fig. 13 : The reasons for the TRUE Test considered unnecessary.

に必須の試験であり「行うことが強く推奨される」と記載されている。しかしながら，アレルゲン入手の煩雑さとその準備の手間や保険点数の低さなどから，あまり積極的に行われていないのが現状で皮膚科医の中でアレルギーに興味があると思われる本学会員を対象にした今回のアンケートでも，パッチテストをよく実施しているのは回答者の28.8%のみであり，約9%はパッチテストを実施していないという結果であった。したがって皮膚科医師全体ではより多くの医師がパッチテストを施行していないものと推測できる。

パッチテストは十分な量のハプテン（アレルゲン）を強制的に経皮吸収させてアレルギー反応を惹起させるため，各々のアレルゲンについて適切な貼布濃度（至適濃度）が設定されている。パッチテストを施行する際には，貼布されるアレルゲンの量や濃度，溶媒となる基剤，貼布に用いるユニットなどに対する知識を要し，得られた反応がアレルギー反応か刺激反応かを判断するためには知識と経験を必要とするため，パッチテストは訓練された皮膚科医が行う必要がある。

わが国では，1994年にジャパニーズスタンダードアレルゲンが設定され[5]，以後日本接触皮膚炎学会の学会員に対してアレルゲンの提供が無償で行われ，スタンダードアレルゲンの陽性率が報告されてきた[5~10]。ジャパニーズスタンダードアレルゲンの陽性率の年次推移をみることは接触皮膚炎の原因の動向をみる上で重要であり，またパッチテスト施行時に，持参品のみではなくスタンダードアレルゲンを貼付することは，問診や臨床所見からは予想できなかった原因物質の特定や，手湿疹や慢性湿疹として漫然と治療されている症例における原因物質の特定，原因製品中のアレルゲンの特定などにおいて有用である。

しかし，現在は薬事法により，学会からのアレルゲン提供が行えない状況にあり，2000年以降は医師が各自でジャパニーズスタンダードアレルゲンを含めた必要なアレルゲンを国内あるいは海外から購入せざるを得ない状況となっている。日本国内では，1995年に鳥居薬品からパッチテスト試薬金属17品目が薬価収載され，翌1996年にパッチテスト試薬（液）10種とパッチテスト試薬（軟膏）13種が薬価収載され，合計40種類のパッチテスト用アレルゲンが販売されている。さらに2009年9月，デンマークのMekos Laboratories ApSからready-to useとなって販売されているパッチテストアレルゲンTRUE Testのうち6種（硫酸ニッケル，重クロム酸カリウム，塩化コバルト，メルカプトベンゾチアゾール，ホルムアルデヒド，チメロサール）が新たに薬価収載され，2010年4月に「パッチテストテープ」という商品名で佐藤製薬から販売された。この製品は，各1種類のアレルゲン一定量を含有した基剤薄層を有するポリエステル支持体の試験片を粘着シートに一体化させてあり，検査施行者は，アレルゲンを被覆してあるラミネートホイルとポリエチレンフィルムをはがして貼付すればよく，これまでのようにアレルゲンをユニットに載せる手間がなく，簡便である。また，すでにアレルゲンを含有している製品であるため，検査施行者によるアレルゲンの量のばらつきやユニットによる反応性や接触面積の違いなどの問題の発生しないアレルゲン製品である。しかしながら，わが国で薬価収載されて販売されたパッチテストテープは1個ずつのアレルゲンで合計6種類のみで，現状の問題点を解決するには至らない。またパッチテストテープの製品規格はアレルゲンを含有する試験片は9×9 mmであるのにそれを固定する粘着テープが50×60.5 mmとなっている。現在頻用されているFinn chamber (Epitest Ltd Oy, Finland) on Scanpor (Alpharma As,Norway) は10個のアレルゲンを12×5 cmの粘着テープで固定し，Haye's Test Chamber (HAL Allergy B.V., the Netherlands) も同様に10個のアレルゲンを12.5 cm×7 cmのテープで固定する規格であるのに比較し，パッチテストテープは1つのアレルゲンを貼付するのに5×6 cmの皮膚を占領するためこの規格では多数のパッチテストテープアレルゲンを患者の背部に貼付するのは難しく，パッチテストテープにおいてはこの点が問題である。

パッチテストテープを含めても国内で販売されているパッチテスト用アレルゲンのみでは，日常診療で経験する多種多様の接触皮膚炎の原因検索には不十分であり，本学会が設定したジャパニーズアレルゲン25種の中で，国内で入手できるのは鳥居薬品のアレルゲン4種のみである。この4種以外のジャパニーズスタンダードアレルゲンは各自が海外から購入しているのが現状で，これらのアレルゲンやパッチテストユニットには薬価収載がないため，パッチテストを施行した場合には1ヵ所について16点（22ヵ所以上は一連で350点のみ）の算定のみである。

佐藤製薬から販売されたパッチテストテープは，

すでに試料がユニットに滴下された状態であり，手間が少なく貼付量の差も少ない製品であり，今後このような ready to use 製品で，少なくともジャパニーズスタンダードアレルゲン 25 種がセットとして薬価収載されて国内で販売されるとより適切なパッチテスト施行頻度が高くなり，患者に有益になると考えられる。

<謝辞>

本アンケートにご協力いただきました日本皮膚アレルギー接触皮膚炎学会会員ならびにパッチテスト試薬 2008 共同研究委員会の先生方に深謝いたします。

文　献

1) 中田土起丈，飯島正文，Maibach HI：金属アレルギーのパッチテストが有効である患者を対象としたパッチテストテープ（硫酸ニッケル，塩化コバルト）の比較臨床試験．臨床医薬．25：937-949，2009
2) 須貝哲郎：TRUE Test と Finn-Chamber の比較．皮膚．30：214-224，1988
3) Sugiura M, Hayakawa R, Kato Y：Patch test results using TRUE Test in Japan. Environ Dermatol. 4：184-188, 1997
4) 高山かおる，横関博雄，松永佳世子他：接触皮膚炎診療ガイドライン．日本皮膚科学会雑誌．19，1757-1793，2009
5) Adachi A：Results of patch tests with standard allergen series of the Research Group of the Japanese Society for Contact Dermatitis in 1994 and annual variations of patients with pigmented contact dermatitis of lichenoid type in 1993. Environ Dermatol. 3：140-150, 1996
6) Miyoshi H：Large-scale patch-testing with Japanese standard series, gold sodium thiosulfate, thimerosal, and mercuric chloride, and the number of new patients with pigmented contact dermatitis in 1994. Environ Dermatol. 4：95-103, 1997
7) Mitsuya K：A multicenter survey of patch testing with Japanese standard series, topical steroid preparations (budesonide, amcinonide and hydrocortisone butyrate) and tin chloride (0.5%, 1.0%, 2.0% pet) in 1997. Environ Dermatol. 6：199-208, 1999
8) Natsuaki M：Results of patch testing with standard allergens of the Japanese Society for Contact Dermatitis and topical nonsteroidal anti-inflammatory preparations in 1998. Environ Dermatol. 7：1-5, 2000
9) Sugiura M：Group study with standard allergen series of the Japanese Society for Contact Dermatitis and gold sodium thiosulfate by patch testing in 1999. Environ Dermatol. 9：105-115, 2002
10) Kurikawa Y：Group study of the optimum concentrations of ketoprofen, tiarofenic acid, suprofe and oxybenzone for the photopatch testing, and the patch test results of the Japanese Standard Allergens and gold sodium thiosulfate in 2000. Environ Dermatol. 9：39-46, 2002

Questionnaire Study on Present Conditions of Patch Testing to the Member of the Japanese Society for Dermatoallergology and Contact Dermatitis in 2010

Kayoko SUZUKI[1], Kayoko MATSUNAGA[2]

[1] *Department of Dermatology, Kariya Toyota General Hospital, 5-15 Sumiyosicho, Kariya, Aichi 448-8505, Japan*
[2] *Department of Dermatology, Fujita Health University School of Medicine, 1-98, Dengakugakubo, Kutsukakecho, Toyoake, Aichi 470-1192, Japan*

Currently, the only commercially available patch test allergens in Japan are 40 allergens by Torii Pharmaceutical Co. and 6 allergens by Sato Pharmaceutical Co. Thus, dermatologists have to purchase many patch test allergens from abroad. In addition, the National Health Insurance (NHI) reimbursement schedule for patch testing remains extremely low. Therefore, when patch testing is performed, a financial loss is incurred.

In light of this situation, a survey regarding patch-testing conditions was conducted among members of the Japanese Society for Dermatoallergology and Contact Dermatitis in February 2010. More than 90% of the dermatologists who responded considered patch testing necessary to diagnose the cause of contact dermatitis, but only 29% performed it routinely, and 62% only occasionally performed patch testing. Overall, 9% of dermatologists did not perform patch testing at all, primarily because of the time and effort involved and difficulty in obtaining allergens. Regarding the current state of patch testing, 97% were dissatisfied with the current practice in Japan, and 90% said the reason for their dissatisfaction was that there are too few patch test allergens commercially available in Japan.

Furthermore, 84% indicated that health insurance coverage for patch testing is a problem; respondents specifically cited low NHI fees as the problem. Regarding the TRUE Test, 98% of dermatologists had no experience with its use, and 82% indicated that if such a ready-to-use patch test allergen product were available, patch testing of patients would increase.

(J Environ Dermatol Cutan Allergol, 5 (2): 91-102, 2011)

Key words : questionnaire study, patch testing, allergen, National Health Insurance (NHI)

ORIGINAL ARTICLE

Comparison of Several Reconstructed Cultured Human Skin Models by Microscopic Observation: Their Usefulness as an Alternative Membrane for Skin in Drug Permeation Experiments

Satoshi Kano[1], Hiroaki Todo[1], Katsunori Furui[1], Kenichi Sugie[1], Yoshihiro Tokudome[1], Fumie Hashimoto[1], Hajime Kojima[3], Kenji Sugibayashi[1,2]

[1]Faculty of Pharmaceutical Sciences and [2]Life Science Research Center, Josai University, Saitama, Japan
[3]National Institute of Health Sciences, Tokyo, Japan

Abstract
Several reconstructed cultured human skin models (RSMs) are already utilized as membrane alternatives to human and animal skin in skin corrosive/irritation tests. They are also utilized in skin permeation experiments from the viewpoint of animal welfare; however, different permeation profiles of chemicals were found between RSMs and excised human or animal skin. RSMs and excised human skin were morphologically evaluated by a light microscope and a transmission electron microscope. In the results, the micromorphology of all RSMs differed from that of human skin. In particular, the lamellar layer between corneocytes in RSMs was much narrower than that in the human stratum corneum. The lamella layer affects not only the diffusion and partition properties of chemical compounds in RSMs but also the concentration-distance profile of chemicals in the models. Furthermore, esterase distribution in RSMs was different to that in human skin. This difference would certainly affect the permeation of both parent ester compounds and their metabolites through RSMs. Evaluation of the morphological and enzymatic differences between RSMs and human skin would be helpful to understand the differences in the chemical permeation profiles between RSMs and human skin.

Key words: reconstructed cultured human skin model, skin permeation, skin morphology, lamella layer

Introduction

Reconstructed (three-dimensional) cultured human skin models (RSMs) are already used as membrane alternatives to human and animal skin in skin permeation experiments. Although the Episkin^{SM} (Skinethic Laboratories, St. Philippe, France) and EpiDerm^{TM} Epi606X (Kurabo Industries Ltd., Osaka, Japan) among RSMs have already been used for skin corrosive/irritation tests of chemical compounds, there are only a few reports on chemical compound permeability through RSMs (Schmook *et al.*, 2001, Watanabe *et al.*, 2001, Netzlaff *et al.*, 2007).

The skin concentration of chemical compounds can be well estimated from skin permeation parameters, which are obtained from the time course of the cumulative amount of the compounds permeating skin (Sugibayashi *et al.*, 2010). Furthermore, skin irritation was found to be fairly related to the skin concentration of chemical compounds (Kano *et al.*, 2006).

These results strongly suggested that evaluation of chemical compound permeation through skin would be necessary to assess the safety of topically applied chemical compounds.

We reported that the skin permeation parameters of chemical compounds were quite different between human skin and RSMs (Kano *et al.*, 2010). Furthermore, esterase activity in skin equivalent TESTSKIN™ LSE-high (Toyobo Co., Ltd., Osaka, Japan) was also different to excised rat skin (Sugibayashi *et al.*, 2004). This difference would affect not only skin permeation but also the skin concentration of ester-containing parent compounds and their hydrolyzed metabolites. In the present study, we investigated histological differences between human skin and RSMs by microscopic observation. Furthermore, carboxylesterase activities and enzyme distribution differences among RSMs were investigated to understand RSM features as an alternative animal membrane to human skin in skin permeation experiments.

Materials and Methods

1. RSMs and excised human skin

TESTSKIN™ LSE-high (LSE-high), EpiDerm™ Epi606X (EpiDerm), Neoderm-E, Vitrolife-skin, LabCyte EPI-model and Episkin℠ (Episkin) were purchased from Toyobo Co., Ltd., Kurabo Industries Ltd., Tego Science Inc. (Seoul, Korea), Gunze Ltd. (Kyoto, Japan), Japan Tissue Engineering Co., Ltd. (Gamagori, Aichi, Japan) and Skinethic Laboratories, respectively. All of these models were used within 3 days after receipt. All experiments were repeatedly conducted with different product lots. Excised abdominal human skin (57 years old, Caucasian female) was purchased from Biopredic International (Rennes, France). The excised human skin experiment was approved by the KAC ethics committee for human-derived products.

2. Hematoxylin and eosin staining of skin section

RSMs and excised human skin were embedded in paraffin wax and continuous sections were prepared at 3 μm thickness using a microtome (Yamato Kohki Industrial Co., Ltd, Saitama, Japan). The specimens were sequentially immersed into xylene, 100%, 90%, 80% and 70% ethanol to remove paraffin. The sections were then stained with hematoxylin and eosin (H.E.) for observation by light microscopy (IX 71; Olympus Co., Tokyo, Japan).

3. Measurement of skin thickness

The H.E.-stained skin sections were observed using a light microscope equipped with a digital camera (DP 72; Olympus Co.), and the thickness of skin sections was measured using DP2-BSW software (Olympus Co.).

4. Observation of lamella structure with a transmission electron microscope

Lamella structures in RSMs were observed by a transmitted electron microscope (TEM) (JEM1200-Ex; Jeol Ltd., Tokyo, Japan). Excised human skin and RSMs were fixed with 0.1% phosphate buffer containing 2% paraformaldehyde and 2% glutaraldehyde, followed by 2 % osmium tetroxide, then with 0.2% ruthenium tetroxide/0.25% potassium hexacyanoferrate. The fixed specimens were embedded in epoxy resin. The skin samples were sectioned at 80–90 nm thickness using an ultramicrotome. The obtained sections were observed by a TEM after double staining with uranil acetate and lead citrate.

5. Observation of skin structure with an *in vivo* confocal laser scanning microscope.

Noninvasive observation of the internal human skin structure was performed *in vivo* by a confocal laser scanning microscope (CLSM) (Vivascope 1500; Lucid Inc., Rochester, NY, U.S.A.) (Sauermann *et al.*, 2002, Hegyi *et al.*, 2009). In the present experiment, RSMs and human skin were observed every 1 μm until 50 μm depth from the membrane surface. The Vivascope 1500 was equipped with an 830 nm wavelength diode laser and water-immersion objective lens (×30). Skin images of 500 × 500 μm were obtained at each observation.

6. Evaluation of skin distribution of esterase enzymes

RSMs and excised human skin were rinsed with pH 7.4 phosphate-buffered saline (PBS) and embedded into Tissue-Tek® OTC compound

(Sakura Finetek Japan Co. Ltd., Tokyo, Japan). These samples were frozen in cold isopentan (2-methyl-butan) at -20 °C. Frozen sections, 20 μm thick, were prepared by a cryostat (CM3050S; Leica Microsystems Ltd., Heerbrugg, Switzerland) and the specimens were observed using a fluorescence microscope (CK40; Olympus Co.) 15 min after application of 1 mL of 0.02 mg/mL fluorescin-5-isothiocyanate diacetate (Wako Pure Chemical Industries, Ltd., Osaka, Japan). The excess solution was washed off with pH 7.4 PBS before observation.

Results

1. Comparison of H.E.-stained skin images

Table 1 shows the thicknesses of RSMs and excised human skin. Each RSM (13.2 ± 4.6 ~ 89.0 ± 1.0 μm) had a thicker stratum corneum than human skin (11.5 ± 6 μm). On the other hand, a thinner viable epidermis and dermis in RSMs (23.3 ± 4.6 ~ 110.1 ± 4.1 μm) was observed than in human skin (474 ± 7.5 μm). Figure 1 compares H.E.-stained images of excised human abdominal skin (Fig. 1a) and RSMs (Fig. 1b-g). Widely separated stratum corneum layers were observed in several H.E.-stained RSMs compared to human skin. The number of cell nuclei stained by hematoxylin in each RSM was lower than in human skin, especially in LSE-high (Fig. 1b) and Neoderm-E (Fig. 1f). Interestingly, many hematoxylin-stained cell nuclei were observed in the stratum corneum in Vitrolife skin (Fig. 1e). This may have been due to inadequate keratinization of keratinocytes.

2. Comparison of lamella structure in stratum corneum observed by a transmission electron microscope

Figure 2 shows TEM images of excised human skin (Fig. 2a) and RSMs (Fig. 2b-g). Lamella layers were frequently observed in human skin (Fig. 2a). Although lamella layers were also found in RSMs (Fig 2b-g), the frequency was relatively lower than in human skin. The lamella layers in LSE-high (Fig. 2b) were narrow and tortuous compared to those in human skin. EpiDerm showed a fairly similar structure (Fig. 2c) to human skin. Neoderm-E (Fig. 2f), LabCyte EPI-model (Fig. 2d) and Episkin (Fig.2g) have aggregated lipid structures and localized lamella analog layers in their intercellular spaces, whereas no lamella layers were observed in Vitrolife skin (Fig. 2e).

Table 1 Skin thickness of excised human skin and reconstituted cultured human skin models.

	Stratum corneum (μm)	Viable epidermis (μm)	Dermis (μm)	Whole skin (μm)
Human	11.5 ± 0.57 (11.8 ± 3.3)[#)]	62.4 ± 3.45 (51.2 ± 12,2)[#)]	412 ± 24.0	493 ± 24.6
LSE-high	29.9 ± 0.93	29.2 ± 2.08	80.8 ± 2.05	136 ± 136
Epiderm	27.0 ± 0.71 12–28 [*)]	53.0 ± 1.15 28–43 [*)]		78.9 ± 78.9
Labcyte EPI-model	89.0 ± 1.00	59.1 ± 0.60	---	149 ± 1.07
Vitrolife skin	13.2 ± 4.61	23.25 ± 4.61	---	38.6 ± 5.23
Neoderm-E	27.8 ± 0.93	23.8 ± 0.87	---	52.2 ± 0.720
Episkin	69.3 ± 1.04 79-102[*)]	28.7 ± 0.92 38-48[*)]	---	99.2 ± 2.58

* Ponec *et al.*, 2000.

\# Sato *et al.*, 1991.

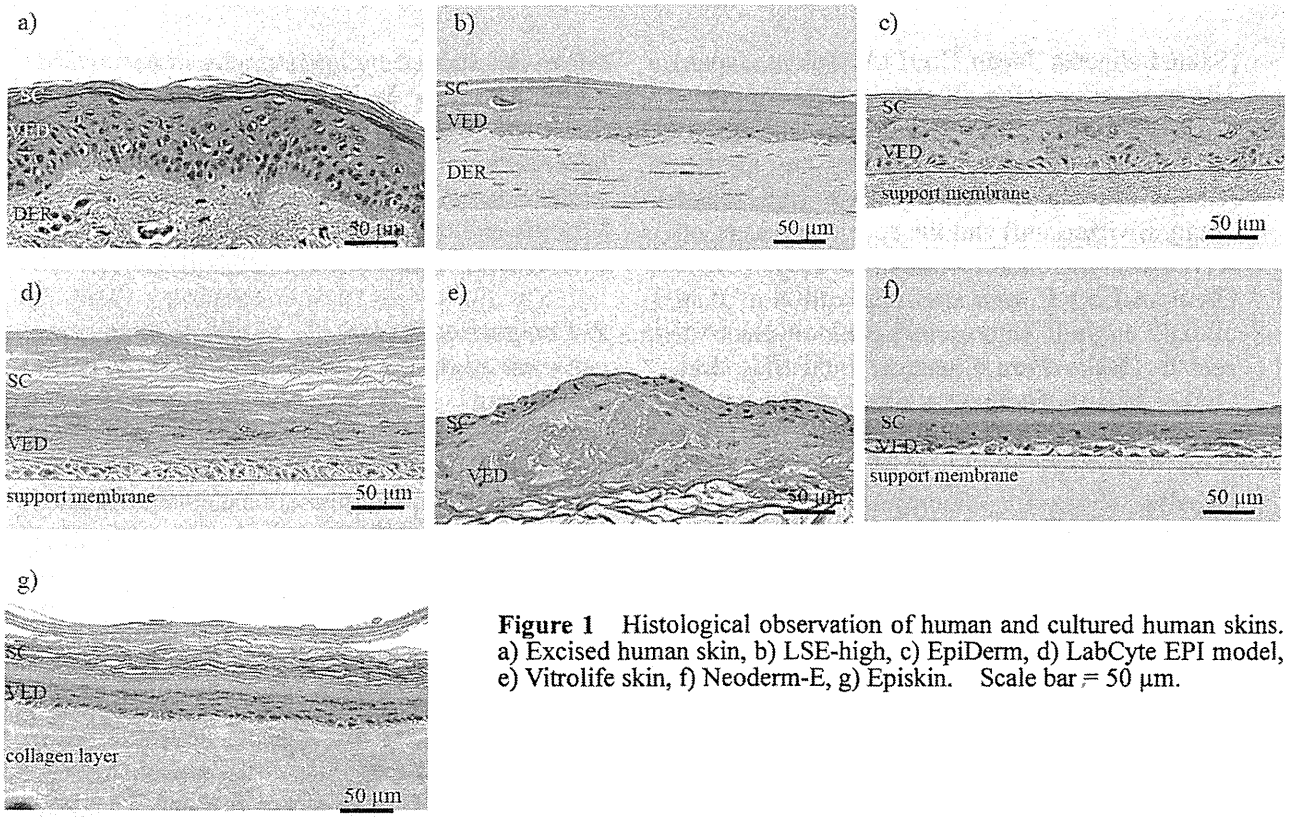

Figure 1 Histological observation of human and cultured human skins. a) Excised human skin, b) LSE-high, c) EpiDerm, d) LabCyte EPI model, e) Vitrolife skin, f) Neoderm-E, g) Episkin. Scale bar = 50 μm.

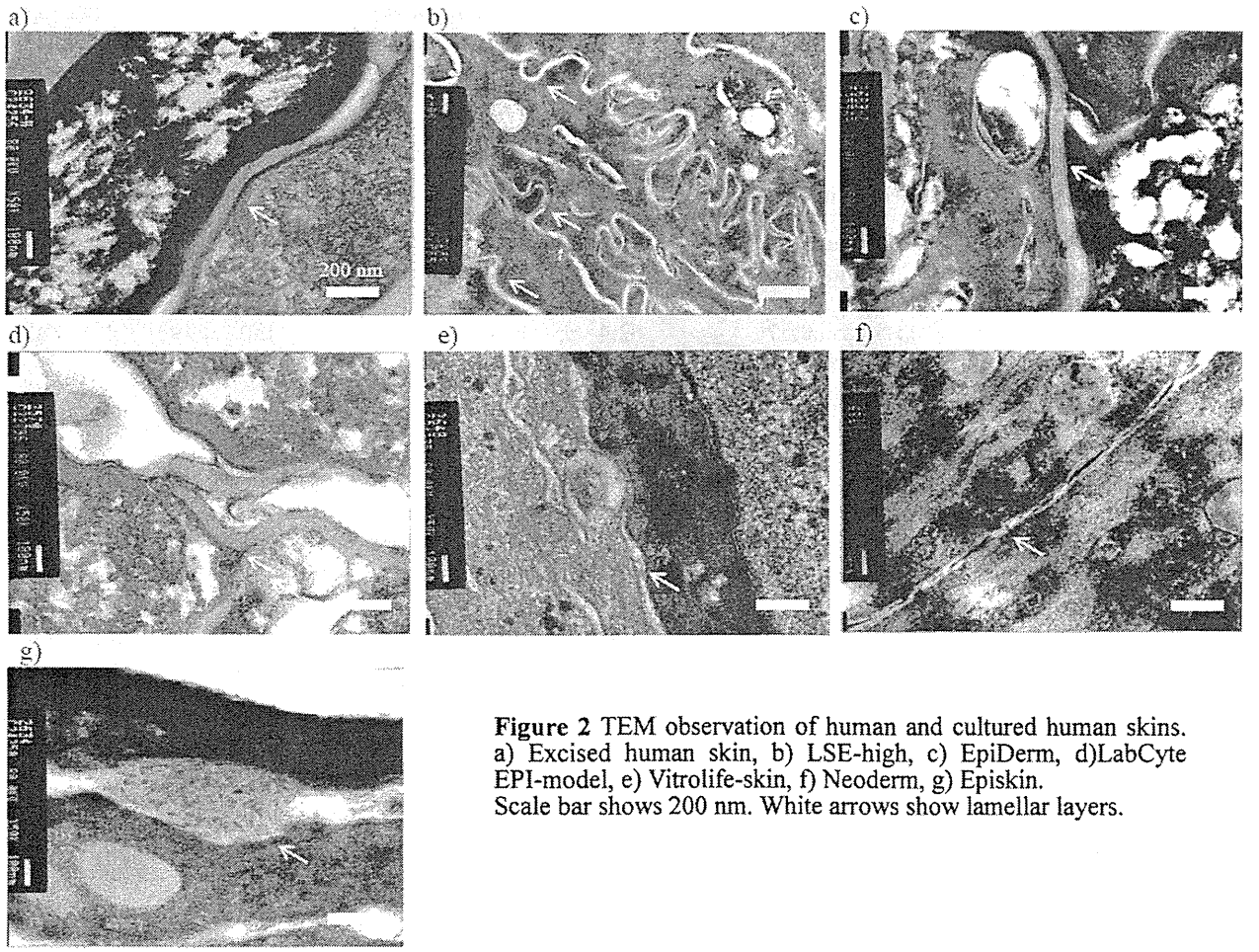

Figure 2 TEM observation of human and cultured human skins. a) Excised human skin, b) LSE-high, c) EpiDerm, d)LabCyte EPI-model, e) Vitrolife-skin, f) Neoderm, g) Episkin. Scale bar shows 200 nm. White arrows show lamellar layers.

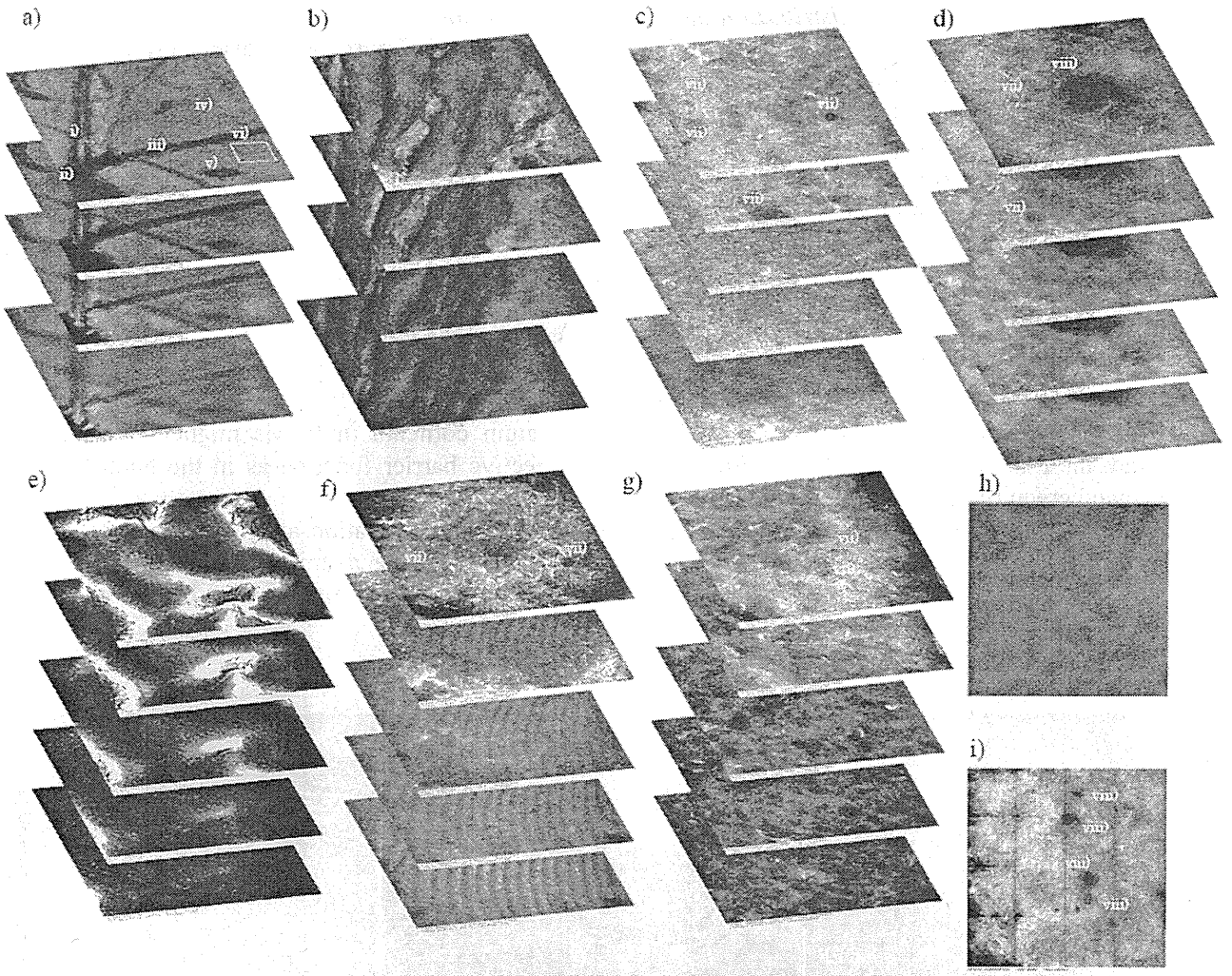

Figure 3 TEM observation of human and cultured human skins. a) Excised human skin, b) LSE-high, c) EpiDerm, d) LabCyte EPI model, e) Vitrolife skin, f) Neoderm-E, g) Episkin, h) Enlargement of vi) area, i) 500 × 500 μm skin images of LabCyte EPI model. Scale bar = 200 nm. i) hair, ii) hair follicle, iii) sulcus cutis, iv) crista cutis, v) sweat gland, vi) corneocyte, vii) corneocyte with nucleus, and viii) pore.

3. Observation of skin structure by an in vitro confocal laser scanning microscope

Figure 3 shows the *in vitro* confocal laser scanning microscope (CLMS) images of human skin (Fig. 3a) and RSMs (Fig. 3b-g). A hair (i), hair follicle (ii), sulcus cutis (iii), crista cutis (iv) and pore (v) were observed in human skin (Fig. 3a) and their sizes gradually diminished by increasing the skin depth. Furthermore, corneocytes ((vi) in Fig. 3a and an enlargement, Fig. 3h) were clearly observed in the shallow part of the human skin (Fig. 3a, h). On the other hand, the sulcus cutis and crista cutis were not confirmed in RSMs (Fig. 3b-g), but the obtained images were different from each other. Corneocytes with a nucleus (vii) were observed in the shallow part of EpiDerm (Fig. 3c), LabCyte EPI model (Fig. 3d), Neoderm-E (Fig. 3f) and Episkin (Fig. 3g), whereas corneocytes were not clearly observed in LSE-high (Fig. 3b) and Vitrolife skin (Fig. 3e). Interestingly, pores (viii) in the skin surface were observed in the LabCyte EPI model (Fig. 3d). The pores were observed until 50 μm from the skin surface in the LabCyte EPI model (Fig. 3d). The surface image (2 mm×2 mm) of the LabCyte EPI model revealed several pores (Fig. 3i). A similar tendency was observed in different lots of the LabCyte EPI model (data not shown).

4. Comparison of esterase distribution between human skin and RSMs.

Figure 4 shows the skin distribution of fluorescein-5-isothiocyanate, a metabolite of fluorescein-5-isothiocyanate diacetate by skin esterase after topical application of fluorescein-5-isothiocyanate. A high intensity of green fluorescence was locally observed in the viable epidermis of excised human skin (Fig. 4a), suggesting that skin esterase scarcely existed in the stratum corneum, but extensively in the viable epidermis. LSE-high, EpiDerm and Episkin showed similar green fluorescence distributions to human skin (Fig. 4b, c and f). On the other hand, the LabCyte EPI model and Vitrolife skin showed green fluorescence not only in the viable epidermis but also in the stratum corneum (Fig. 4d and e).

Discussion

H.E.-stained skin sections revealed that the skin thicknesses of the stratum corneum, viable epidermis and dermis in the RSMs were different to those in the human skin. The outmost layer of skin, the stratum corneum, is the biggest barrier against the entry of exogenous substances, so its thickness might affect the skin permeation rate of chemical compounds (Barry *et al.*, 1983). Although RSMs have a thicker stratum corneum than excised human skin, RSMs generally show faster skin permeation of chemical compounds (Kano *et al.*, 2010). The shallow part of the stratum corneum in RSMs might not have an effective barrier function as in the human stratum corneum.

TEM observation and CLSM results show that RSMs have a unique structure in the inter-corneocytes. Partition and diffusion parame-

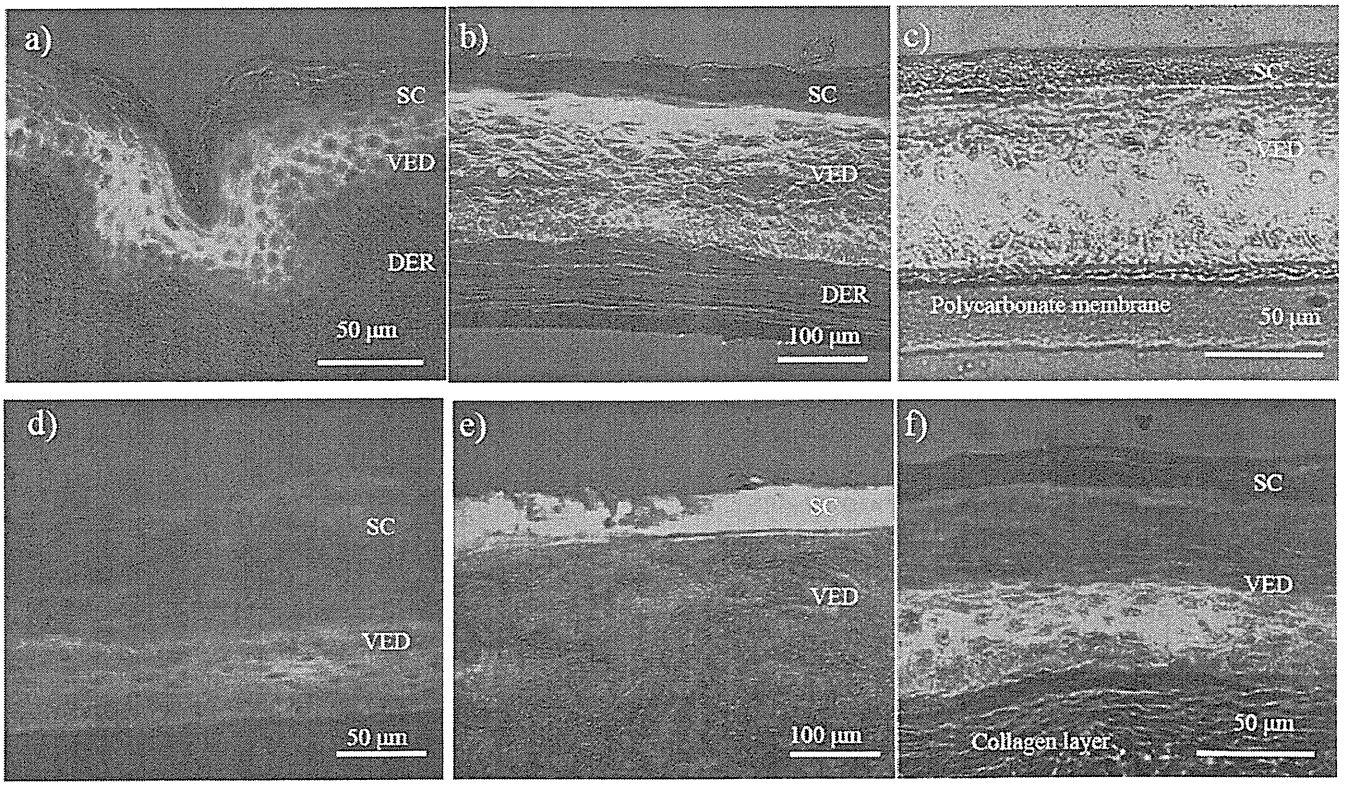

Figure 4 Fluorescein observation of human and cultured human skins 15 min after application of fluorescin-5-isothiocyanate diacetate. a) Excised human skin, b) LSE-high, c) EpiDerm, d) LabCyte EPI model, e) Vitrolife skin, f) Episkin. Scale bar = 200 nm. Abbreviations: SC: stratum corneum, VED: viable epidermis, DER: dermis.

ters of chemical compounds topically applied to RSMs were much different from human skin (Kano *et al.*, 2010). The diffusion and partition parameters depend on the diffusivity of the chemical compounds in the stratum corneum and lipophilicity of the stratum corneum, respectively. Inter-corneocyte space is filled with ceramides and other lipids to compose the lamella structure (Elias *et al.*, 1975, Lampe *et al.*, 1983). Therefore, the maturity of the lamellar structure and content of lipid or constitution of intercellular lipids in the stratum corneum would affect the diffusion and partition parameters of topically applied compounds. The localized distribution and frequency of lamella layers were observed in several RSMs. These results might also relate to the different partition parameters in RSMs. Furthermore, observation using the Vivascope 1500 revealed pores in several RSMs. These RSMs might be difficult to use in skin permeation experiments in the present state because these models have different lipophilicity to human skin. The results were not fully analyzed with a small-angle X-ray diffraction analyzer in the present study. Further experiments will be needed to elucidate the lamella structure differences between excised human skin and RSMs.

Investigation of the total amount of metabolic enzymes (Luu-The *et al.*, 2009, Hu *et al.*, 2010) and their distribution in skin is very important because the difference in the metabolic enzyme activity and distribution between human skin and RSMs would affect not only the skin distribution of metabolites but also to their efficacy or toxicity; however, only a few studies have been carried out on the enzyme distribution in RSMs. Thus, evaluation of enzyme distribution is necessary in RSMs. The skin distribution of fluorescin-5-isothiocyanate revealed that each RSM had a different enzyme distribution, suggested that the parent and its metabolite concentration-distance profiles in each RSM would be different. Esterase is expressed in the granular layer of the epidermis (Clark *et al.*, 1993, Jewell *et al.*, 2007, Zhu *et* al., 2007); however, the Vivascope 1500 revealed denucleated corneocytes in the shallow part of EpiDerm, the LabCyte EPI model Neoderm-E and Episkin. These undifferentiated cells would affect esterase activity. Evaluation of the amount of esterase activity in RSMs will be needed to use them as a membrane alternative to skin in skin permeation experiments.

Conclusion

The present histological observation suggested that structural differences in RSMs could be the reason for skin permeation differences among RSMs; however, chemical compound permeation through human skin could be predicted from rat or porcine skin despite their different structures. Therefore, combination analysis of skin permeation and histological results would be extremely effective to clarify the characteristics of each RSM. We believe that understanding the characteristics of RSMs is very important for more widespread usage of RSMs.

Acknowledgements

Preparation of skin specimens and TEM observations were conducted by Hanaichi Ultrastructure Research Institute (Okazaki, Aichi, Japan). H.E.-stained samples were prepared by Genostaff Co., Ltd. (Tokyo, Japan). Part of the present study was supported by a Grant-in-Aid for Scientific Research (H22-iyaku-ippan-002) from the Ministry of Health, Labor, and Welfare, Japan.

References

Barry B.W., Dermatological formulations: Percutaneous absorption, Marcel Dekkrer, New York and Basel, 1983.

Clark N.W., Scott R.C., Blain P.G., Williams F.M. (1993) Fate of fluazifop butyl in rat and human skin in vitro, *Arch. Toxicol.*, **67**, 44-48.

Elias P.M., Friend D.S. (1975) The permeability barrier in mammalian epidermis, *J. Cell. Biol.*, **65**, 180-191.

Kano, S., Todo, H., Sugie, K., Fujimoto, H., Nakada, K., Tokudome, Y., Hashimoto, F. and Sugibayashi, K. (2010) Utilization of reconstructed cultured human skin models as an alternative skin for permeation studies of chemical compounds, *Altern. Animal Test. Experiment.*, **15**, 61-70.

Kano, S. and Sugibayashi, K. (2006) Kinetic analysis on the skin disposition of cytotoxicity as an index of skin irritation produced by cetylpyridinium chloride: Comparison of in vitro data using a three-dimensional cultured human skin model with in vivo results in hairless mice, *Pharm Res*, **23**, 329-335.

Hegyi, J., Hegyi, V., Messer, G., Arenberger, P., Ruzicka, T. and Berking, C. (2009) Confocal laser-scanning capillaroscopy: a novel approach to the analysis of skin capillaries in vivo, *Skin Res. Technol.*, **15**, 476-481.

Hu, T., Khambatta, Z.S., Hayden, P.J., Bolmarcich, J., Binder, R.L., Robinson, M.K., Carr, G.J., Tiesman, J.P., Jarrold, B.B., Osborne, R., Reichling, T.D., Nemeth, S.T. and Aardema, M.J. (2010) Xenobiotic metabolism gene expression in the EpiDermin vitro 3D human epidermis model compared to human skin, *Toxicol In Vitro*, **24**, 1450-1463.

Jewell C., Prusakiewicz J.J., Ackermann C., Payne N.A., Fate G., Voorman R, Williams F.M. (2007) Hydrolysis of a series of parabens by skin microsomes and cytosol from human and minipigs and in whole skin in short-term culture, *Toxicol. App. Pharmacol.*, **225**, 221-228.

Lampe M.A., William M.L., Elias P.M. (1983) Human epidermal lipids: characterization and modulation during differentiation, *J. Lipid Res.*, **24**, 131-140.

Luu-The, V., Duche, D., Ferraris, C., Meunier, J.R., Leclaire, J. and Labrie, F. (2009) Expression profiles of phases 1 and 2 metabolizing enzymes in human skin and the reconstructed skin models Episkin and full thickness model from Episkin, *J Steroid Biochem Mol Biol*, **116**,178-186.

Netzlaff, F., Kaca M., Bock, U., Haltner-Ukomadu, E., Meiers, P., Lehr, C.M. and Schaefer, U.F. (2007) Permeability of the reconstructed human epidermis model Episkin in comparison to various human skin preparations, *Eur. J. Pharm. Biopharm.*, **66**, 127-134.

Ponec M., Boelsma E., Weerheim A., Mulder A., Bouwstra J., Mommaas M. (2000) Lipid and ultrastructural characterization of reconstructed skin models, *Int. J. Pharm.*, **203**, 211-225.

Sato K., Sugibayashi K., Morimoto Y. (1991) Species difference in percutaneous absorption of nicorandil, *J. Pharm. Sci.*, **80**, 104-107.

Sauermann, K., Clemann, S., Jaspers, S., Gambichler, T., Altmeyer, P., and Hoffmann K. (2002) Age related changes of human skin investigated with histometric measurements by confocal laser scanning microscopy in vivo, *Skin Res. Technol.*, **8**, 52-56.

Schmook F.P., Meingassner J.G., Billich A. (2001) Comparison of human skin or epidermis models with human and animal skin in in-vitro percutaneous absorption, *Int. J. Pharm.*, **215**, 51-56.

Sugibayashi, K., Todo, H., Oshizaka, T. and Owada, Y. (2010) Mathematical model to predict skin concentration of drugs: toward utilization of silicone membrane to predict skin concentration of drugs as an animal testing alternative, *Pharm. Res.*, **27**, 134-142.

Watanabe T., Hsegawa T., Takahashi H., Ishibashi T., Takayama K., Sugibayashi K. (2001) Utility of the three-dimensional cultured human skin model as a tool to evaluate skin permeation of drugs, *Altern. Animal Test. Experiment.*, **8**, 1-14.

Zhu Q.G., Hu J.H., Liu J.Y., Lu S.W., Liu Y.X., .Wang J. (2007) Stereoselective Characteristics and Mechanisms of Epidermal Carboxylesterase Metabolism Observed in HaCaT Keratinocytes, *Biol. Pharm. Bull.*, **30**, 532-536.

(Received: May 18/
Accepted: October 25)

Corresponding author:
Kenji Sugibayashi, Ph.D.,
Faculty of Pharmaceutical Sciences and
Life Science Research Center, Josai University,
1-1 Keyakidai, Sakado, Saitama 350-0295, Japan
Tel.:+81-49-271-7367;
Fax:+81-49-271-8137;
Email: sugib@josai.ac.jp

Phytochemistry 72 (2011) 1814–1820

Contents lists available at ScienceDirect

Phytochemistry

journal homepage: www.elsevier.com/locate/phytochem

In vitro photochemical and phototoxicological characterization of major constituents in St. John's Wort (*Hypericum perforatum*) extracts

Satomi Onoue [a,*], Yoshiki Seto [a], Masanori Ochi [a], Ryo Inoue [a], Hideyuki Ito [b], Tsutomu Hatano [b], Shizuo Yamada [a]

[a] *Department of Pharmacokinetics and Pharmacodynamics and Global Center of Excellence (COE) Program, School of Pharmaceutical Sciences, University of Shizuoka, 52-1 Yada, Suruga-ku, Shizuoka 422-8526, Japan*

[b] *Division of Pharmaceutical Sciences, Okayama University, Graduate School of Medicine, Dentistry and Pharmaceutical Sciences, 1-1-1 Tsushimanaka, Kita-ku, Okayama 700-8530, Japan*

ARTICLE INFO

Article history:
Received 15 July 2010
Received in revised form 9 March 2011
Available online 23 July 2011

Keywords:
St. John's Wort
Guttiferae
In vitro phototoxicity
Reactive oxygen species
Singlet oxygen
Superoxide

ABSTRACT

Extracts from St. John's Wort (SJW: *Hypericum perforatum*) have been used for the treatment of mild-to-moderate depression. In spite of the high therapeutic potential, orally administered SJW sometimes causes phototoxic skin responses. As such, the present study aimed to clarify the phototoxic mechanisms and to identify the major phototoxins of SJW extract. Photobiochemical properties of SJW extract and 19 known constituents were characterized with focus on generation of reactive oxygen species (ROS), lipid peroxidation, and DNA photocleavage, which are indicative of photosensitive, photoirritant, and photogenotoxic potentials, respectively. ROS assay revealed the photoreactivity of SJW extract and some SJW ingredients as evidenced by type I and/or II photochemical reactions under light exposure. Not all the ROS-generating constituents caused photosensitized peroxidation of linoleic acid and photodynamic cleavage of plasmid DNA, and only hypericin, pseudohypericin, and hyperforin exhibited *in vitro* photoirritant potential. Concomitant UV exposure of quercitrin, an SJW component with potent UV/Vis absorption, with hyperforin resulted in significant attenuation of photodynamic generation of singlet oxygen from hyperforin, but not with hypericin. In conclusion, our results suggested that hypericin, pseudohypericin, and hyperforin might be responsible for the *in vitro* phototoxic effects of SJW extract.

1. Introduction

Drug-induced phototoxicity is characterized by an inflammatory reaction of the skin after topical or systemic administration of pharmaceutical substances (Moore, 2002; Onoue et al., 2009a). Several classes of drugs including antibacterials, thiazide diuretics, non-steroidal anti-inflammatory drugs, quinolones, and tricyclic antidepressants, despite being non-toxic by themselves, may become reactive under exposure to environmental light, leading to undesired side-effects (Moore, 2002). There are at least three types of drug-induced phototoxic skin reactions, including photoirritant, photogenotoxic, and photoallergic skin responses, the mechanisms and pathologic features of which are quite different. A number of efforts have been made to design efficacious screening systems for predicting the phototoxic and photoreactive potential of new drug entities (Onoue et al., 2009a), with the aim of avoiding these undesired side effects.

Previously, our group proposed high-throughput screening systems to predict the phototoxic risk of newly synthesized drug candidates, which include a reactive oxygen species (ROS) assay (Onoue et al., 2008b,d; Onoue and Tsuda, 2006) and a derivative of reactive oxygen metabolites (D-ROM) assay (Onoue et al., 2010) for predicting phototoxic potential, capillary gel electrophoresis-based photocleavage assay (Onoue et al., 2008a), and DNA-binding assay (Onoue et al., 2009b) for photogenotoxic risk. In particular, the ROS assay was designed for predicting the phototoxicity and/or photosensitivity of the tested chemicals on the basis of ROS generation from photo-irradiated chemicals. According to the 1st law of photochemistry, the primary trigger for photochemical and photobiological reactions of phototoxins is the absorption of UV and visible (Vis) light ranging from 290 to 700 nm (Onoue et al., 2009a). Molecular oxygen, a triplet radical which is in its ground state, appears to be the predominant acceptor of excitation energy as its lowest excited level (singlet state) has a comparatively low value. Energy transfer from excited triplet photosensitizer to the oxygen (type II photochemical reaction) could thus produce excited singlet oxygen. Electron or hydrogen transfer could lead to the formation of free radical species (type I

* Corresponding author. Tel.: +81 54 264 5633; fax: +81 54 264 5635.
E-mail address: onoue@u-shizuoka-ken.ac.jp (S. Onoue).

0031-9422/$ - see front matter © 2011 Elsevier Ltd. All rights reserved.
doi:10.1016/j.phytochem.2011.06.011

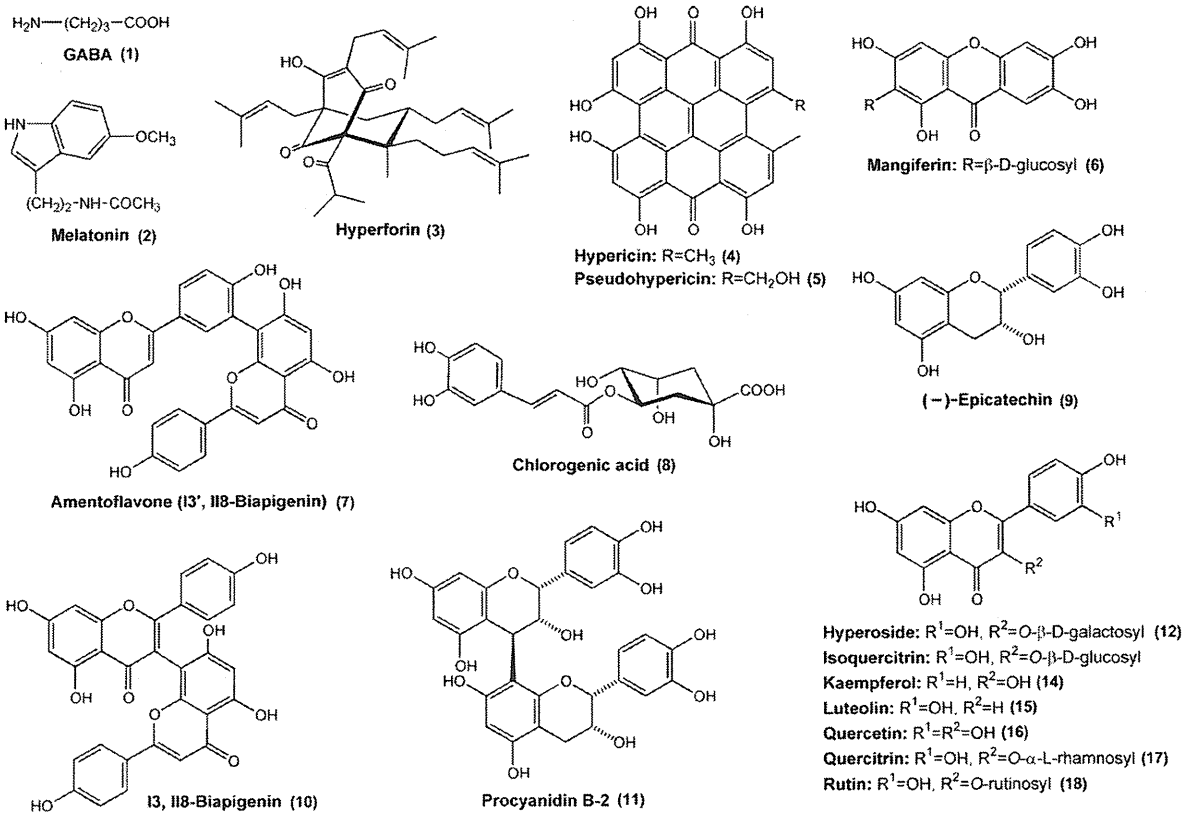

Fig. 1. Structures of major constituents in SJW extract.

photochemical reaction). Currently, these radical species are identified as the principal intermediate species in phototoxic responses (Foote, 1991), so that the generation of ROS from irradiated chemicals is indicative of phototoxic potential.

Recently, with roughly one report per 300,000 cases treated with extract of St. John's Wort (SJW: *Hypericum perforatum*), reversible phototoxic skin reactions, such as delayed erythema, blistering, and hyperpigmentation, are the most common pharmacovigilance case reports documented (Schulz, 2001). SJW extract has been used to treat a variety of conditions, especially psychovegetative disorders, depressive disorders, anxiety, and/or nervous agitation (Linde, 2009). The main bioactive components of SJW extract for treatment of depression were thought to be hypericin (**4**) and hyperforin (**5**) (Fig. 1) (Lawvere and Mahoney, 2005), although recent studies demonstrated that flavonoids might also be more important for antidepressant activity (Nahrstedt and Butterweck, 2010). Numerous studies have demonstrated the pharmacokinetic interaction between SJW extract and other drugs, the mechanisms of which involve the drug-metabolizing enzyme CYP3A4 activated by hyperforin (**5**) (Nahrstedt and Butterweck) and the transport protein P-glycoprotein (Schulz, 2006). In contrast, the phototoxic potential and detailed mechanism of the SJW extract have been studied less extensively. Although hypericin (**4**) and its related metabolites are believed to cause severe photosensitization, known as hypericism (Siegers et al., 1993; Vandenbogaerde et al., 1998; Yu et al., 1996), further phototoxic constituents remain to be indentified and their structures elucidated.

The main purpose of the present investigation is to characterize the *in vitro* photochemical and phototoxicological properties of major SJW components, which may allow for the identification of phototoxic components in SJW. A better understanding of the *in vitro* photochemical properties of the components would be key for the safer use of SJW extract. The ROS assay was carried out for SJW extract and 19 SJW constituents, which include amino acids, flavonoids, naphthodianthrones, phenylpropanes, phloroglucinols, and xanthones (Fig. 1). The photoreactive components of SJW with potent ROS generation were further characterized with a focus on the *in vitro* photoirritant and/or *in vitro* photogenotoxic potential. Furthermore, possible photochemical interactions between phototoxic and anti-oxidative constituents were assessed by the ROS assay.

2. Results and discussion

2.1. ROS assay on SJW extract and major components

In the present study, ROS assays were carried out on the SJW extract for photobiochemical characterization. The exposure of the SJW extract (100 μg/mL) to simulated sunlight (250 W/m^2), consisting of UVA/B and Vis light, led to the marked production of ROS, such as singlet oxygen (Fig. 2A) and superoxide (Fig. 2B), in a time-dependent manner. No significant generation of ROS was seen without UV irradiation (data not shown). For comparison, naproxen and erythromycin, typical phototoxic and non-phototoxic chemicals, respectively, were also assessed using the ROS assay. As shown in Fig. 2, naproxen had an ability to generate both singlet oxygen and superoxide under light exposure, although ROS generation from irradiated erythromycin was negligible.

For further characterization, photochemical properties of 19 major constituents of SJW extract were also assessed by the ROS assay (Table 1). Some SJW constituents at a concentration of 20 μM tended to generate singlet oxygen, superoxide, or both when exposed to UV/Vis light for 60 min, which included

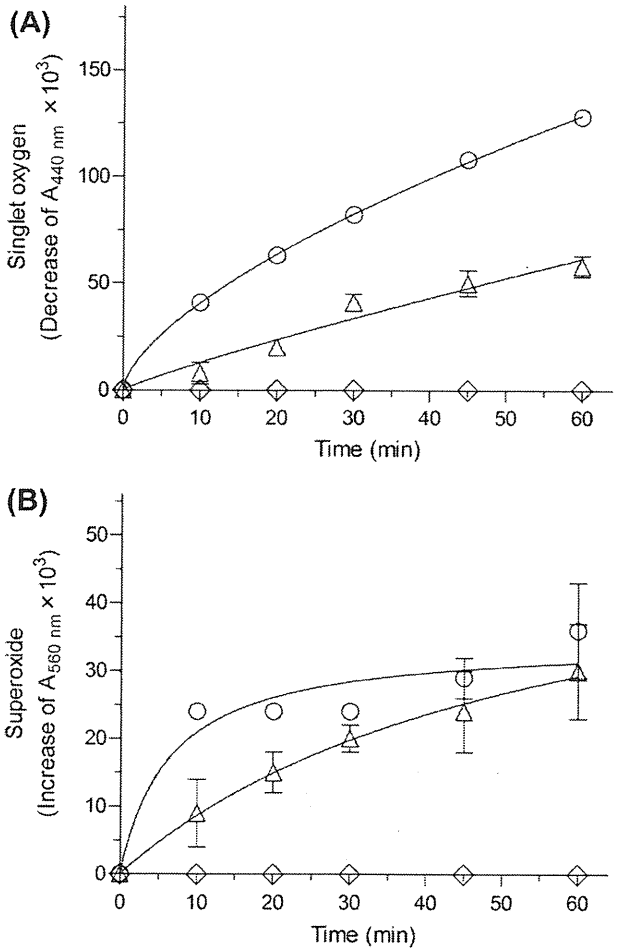

Fig. 2. Generation of singlet oxygen (A) and superoxide (B) from SJW extract irradiated with simulated sunlight. Each sample was dissolved in 20 mM NaPB (pH 7.4) and exposed to simulated sunlight for the indicated periods with an irradiance of 250 W/m^2. ○, SJW extract at 100 μg/mL; △, naproxen at 20 μM; and ◇, erythromycin at 20 μM. Data represent mean ± SD of three determinations.

Table 1
Generation of ROS from photo-irradiated chemicals.

Chemicals	ROS generation		Content (%)*
	Singlet oxygen ($\Delta A_{440\ nm} \times 10^3$)	Superoxide ($\Delta A_{560\ nm} \times 10^3$)	
SJW extract (100 μg/mL)	128 ± 3	36 ± 7	–
SJW constituents (20 μM)			
Amino acid derivatives			
GABA (**1**)	18 ± 6	8 ± 9	2.1
Melatonin (**2**)	49 ± 8	3 ± 2	<0.01
Biflavones			
I3,II8-Biapigenin (**10**)	107 ± 12	4 ± 2	0.98
I3′,II8-Biapigenin (Amentoflavone) (**7**)	107 ± 22	19 ± 14	0.080
Catechins			
Catechin	15 ± 8	N.D.	0.27
Epicatechin (**9**)	10 ± 3	N.D.	0.23
Flavonols/Flavones			
Hyperoside (**12**)	N.D.	N.D.	0.60
Isoquercitrin (**13**)	47 ± 10	N.D.	0.32
Kaempferol (**14**)	72 ± 18	15 ± 13	0.018
Luteolin (**15**)	108 ± 7	N.D.	0.061
Quercetin (**16**)	150 ± 11	N.D.	0.83
Quercitrin (**17**)	4 ± 8	N.D.	0.32
Rutin (**18**)	26 ± 4	N.D.	0.22
Naphthodianthrones			
Hypericin (**4**)	134 ± 4	24 ± 6	0.12
Pseudohypericin (**5**)	128 ± 18	5 ± 4	0.49
Phenylpropanoids			
Chlorogenic acid (**8**)	N.D.	N.D.	0.26
Phloroglucinols			
Hyperforin (**3**)	86 ± 2	N.D.	3.8
Proanthocyanidins			
Procyanidin B-2 (**11**)	117 ± 5	N.D.	0.37
Xanthones			
Mangiferin (**6**)	36 ± 7	29 ± 5	0.11
Pharmaceuticals (20 μM)			
Non-phototoxic drug			
Erythromycin	N.D.	N.D.	–
Phototoxic drugs			
Naproxen	54 ± 3	29 ± 8	–
Quinine	211 ± 3	4 ± 11	–

Each sample was dissolved in 20 mM NaPB (pH 7.4) and exposed to UVA/B and Vis light (250 W/m^2) for 60 min. Data represent mean ± SD for three independent experiments.
* Content of each constituents in the tested SJW extract.

I3,II8-biapigenin (**10**), I3′,II8-biapigenin (amentoflavone) (**7**), kaempferol (**14**), luteolin (**15**), quercetin (**16**), hypericin (**4**), pseudohypericin (**5**), hyperforin (**3**), and procyanidin B-2 (**11**). On the basis of the ROS data, the photoreactivity of these chemicals was found to be much higher than that of naproxen. These data were partly consistent with previous observations showing the phototoxic potential of hypericin (**4**) and hyperforin (**3**) (Lawvere and Mahoney, 2005). Quercetin (**16**) and procyanidin (**11**) B-2 were identified to be potent photoreactive chemicals; however, not all flavonoids exhibited significant ROS generation under light exposure. In particular, there appeared to be marked differences in photoreactivity between the glycoside and the aglycone moieties, as evidenced by the ROS data on quercetin (**16**) and its glycosides such as hyperoside (**12**), quercitrin (**17**), isoquercitrin (**13**), and rutin (**18**). No significant ROS generation was seen for γ-amino-*n*-butyric acid (GABA) (**1**), catechins (**9**), hyperoside (**12**), quercitrin (**17**), and chlorogenic acid (**8**), suggesting less photosensitivity.

2.2. Photodynamic lipid peroxidation induced by irradiated SJW constituents

On the basis of the ROS assay, some natural products from the SJW extract were deduced to be photoreactive and/or phototoxic mainly via type II photochemical reaction. These findings, taken together with their concentrations (>0.05%) in the SJW extract as determined by UPLC/ESI-MS analysis (Table 1), prompted us to clarify the *in vitro* phototoxic potential of some photoreactive SJW constituents in more detail, which include I3,II8-biapigenin (**10**), I3′,II8-biapigenin (**7**), luteolin (**15**), quercetin (**16**), hypericin (**4**), pseudohypericin (**5**), hyperforin (**3**), and procyanidin B-2 (**11**). Peroxidation of fatty acids can be used for predicting the *in vitro* photoirritant potential of pharmaceutical and nutraceutical products. In the present study, we attempted to investigate the ability of SJW constituents to photosensitize peroxidation of linoleic acid (Fig. 3). To evaluate and compare the lipid peroxide level, malondialdehyde (MDA), a secondary product of lipid peroxidation, was determined by the thiobarbituric acid (TBA) method (Ohkawa et al., 1979). UV irradiation of linoleic acid (1 mM) without photosensitizers resulted in slight formation of peroxidation products (260 nM); however, irradiation in the presence of phototoxins (200 μM) such as naproxen and quinine produced a much greater amount of the products (ca. 700 nM). In contrast, the addition of erythromycin did not lead to enhanced lipid peroxidation under the present experimental conditions, which was consistent with the results from the ROS assay. With respect to the photoreactive chemicals in the SJW extract, only hypericin (**4**),

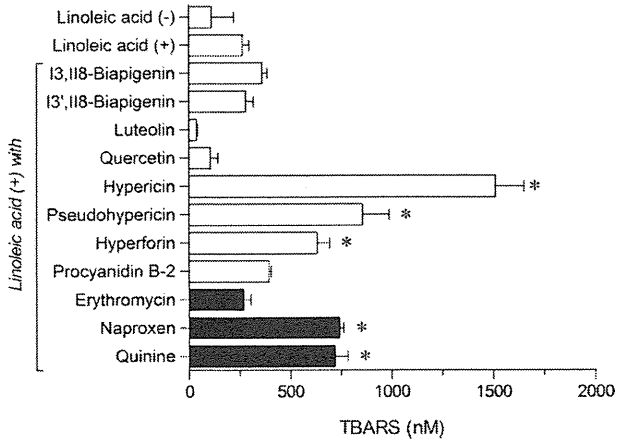

Fig. 3. *In vitro* lipid peroxidation induced by photo-irradiated SJW constituents and pharmaceutical chemicals. Linoleic acid (10^{-3} M) and tested chemicals (200 μM) were dissolved in 20 mM NaPB (pH 7.4) containing 0.05% Tween 20, and then exposed to simulated sunlight (250 W/m^2) for 1 h. Lipid peroxidation was measured using a TBA assay, and a standard curve of 1,1,3,3-tetraethoxypropane was used to quantitate the amount of TBA-reactive substance (TBARS) produced. Linoleic acid (+) or (−) indicates the linoleic acid with or without UVA/B irradiation, respectively. Data represent mean ± SD of three determinations. *$P < 0.05$ with respect to the linoleic acid (+).

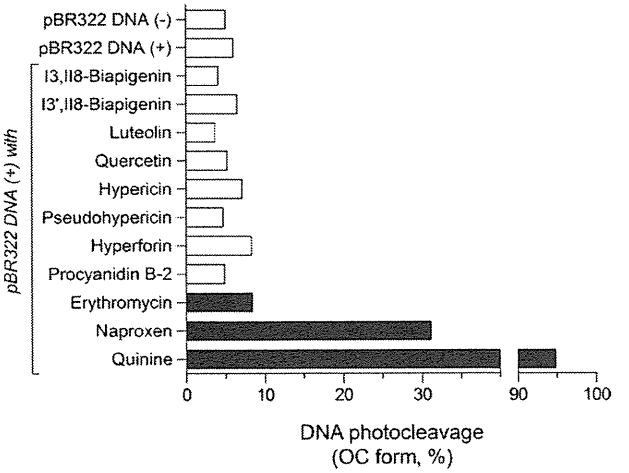

Fig. 4. *In vitro* DNA-photocleavage assay for predicting photogenotoxic potential. Supercoiled form of pBR322 DNA was exposed to simulated sunlight (250 W/m^2) for 25 min with or without SJW constituents or pharmaceutical chemicals (200 μM). Each pBR322 DNA sample was separated on 0.8% agarose gel and stained with ethidium bromide. According to AGE analysis, the photodynamic impairment of pBR322 DNA is expressed as % of open circular (OC) form. pBR322 DNA (+) or (−) indicates the pBR322 DNA with or without UVA/B irradiation, respectively.

pseudohypericin (**5**), and hyperforin (**3**) at a concentration of 200 μM exhibited significant lipid peroxidation with generated MDA of 1510 ± 140, 857 ± 227, and 630 ± 62 nM, respectively. However, these constituents at 20 μM had no ability to oxidize linoleic acid under light exposure (data not shown). Slight increase in lipoperoxide level was also observed with procyanidin B-2 (**11**), whereas two flavonoids tended to attenuate UV-evoked auto-oxidation of linoleic acid. There appeared to be a data discrepancy between results from the ROS and TBA assays on these flavonoids. However, the lack of lipoperoxidating activities was not unexpected because these flavonoids also have anti-oxidative activities due to their phenolic OH groups (Seelinger et al., 2008). Given these findings, some photoreactive SJW constituents, including hypericin (**4**), pseudohypericin (**5**) and hyperforin (**3**), at high concentration exhibited *in vitro* photoirritant potential.

2.3. Photogenotoxic potential of SJW constituents

It is well established that DNA strand breaks cause the structural conversion of supercoiled pBR322 DNA (SC) to the open circular (OC) form (Viola et al., 2000), so that the structural conversion of irradiated pBR322 DNA in the presence of phototoxins can be indicative of *in vitro* photogenotoxic risk. The photosensitized DNA cleavage products were analyzed by agarose gel electrophoresis (AGE), using ethidium bromide (EtBr) as an intercalating dye (Fig. 4). According to the AGE data on the intact pBR322 DNA, most DNA displayed the supercoiled form (ca. 95%), and irradiation of the pBR322 DNA alone with UVA/B and Vis light (250 W/m^2) for 25 min did not result in impairment of DNA. However, addition of phototoxins such as naproxen and quinine led to marked damage to pBR322 DNA; in particular, the majority of irradiated DNA with quinine existed in the open circular form (ca. 95%). Interestingly, there were no significant structural transitions of pBR322 DNA in the presence of photoreactive SJW components, even hypericin (**4**) and hyperforin (**3**). Previously, capillary gel electrophoretic studies also demonstrated that some ROS-generating phototoxins, including indomethacin and piroxicam, failed to cause DNA damage in similar experimental conditions (Onoue et al., 2008a). In drug-induced photogenotoxic cascades, solar radiation basically causes genotoxic effects by two mechanisms: either directly by photoexcitation of DNA or indirectly by excitation of photosensitizers (Alderfer et al., 1993). For both mechanisms, interaction between DNA and phototoxins is thought to be necessary in the early stage of photogenotoxic cascades (Onoue et al., 2009b). In this context, there is a probability that the tested photoreactive chemicals from SJW extract have no affinity with DNA molecules, and the *in vitro* photogenotoxic potential of these SJW constituents might not be serious.

2.4. Potential suppression of in vitro phototoxicity by co-existing SJW component

Wilhelm and co-workers previously demonstrated that quercitrin (**17**) was effective to control the *in vitro* phototoxic activity of the SJW extract; however, the detailed mechanisms remain unclear (Wilhelm et al., 2001). Schmitt and co-workers also suggested that hypericin (**4**) combined with either SJW extracts or constituents might exert less phototoxicity than pure hypericin (**4**) (Schmitt et al., 2006). These findings could provide a working hypothesis that quercitrin (**17**) and other photochemically inactive components with potent UV absorption affect the *in vitro* photochemical and phototoxicological behavior of photoreactive constituents, resulting in potential suppression of the *in vitro* phototoxic risk of SJW extract.

To clarify the possible interaction among these constituents, *in vitro* photochemical studies were carried out with focus on UV-absorbing properties and ROS-generating abilities (Fig. 5). According to the UV spectral patterns obtained (Fig. 5A), each natural product was found to be a strong UV absorber; in particular, hypericin (**4**) showed intense absorption in the Vis range, as well as for UVA/B light. Therefore, they may absorb photon energy and be excited upon exposure to sunlight; however, quercitrin (**17**) was found to be less photoreactive as evaluated by the ROS assay. Theoretically, quercitrin (**17**) might act as a potent UV absorber to suppress solar-evoked photoactivation of phototoxic natural products in the body, although most quercitrin (**17**) would undergo metabolism. Alternatively, quercitrin (**17**) might work directly as an anti-oxidant as reported previously (Zou et al., 2004), being partly associated with regulation of *in vitro* phototoxic

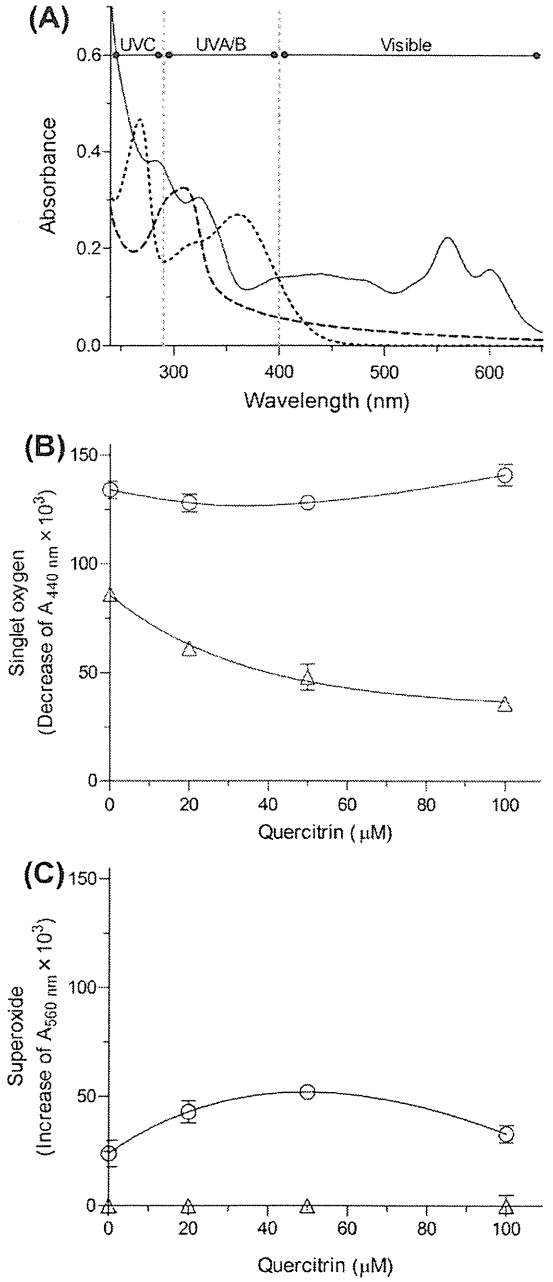

Fig. 5. *In vitro* photochemical interaction among SJW constituents. (A) UV spectra of SJW constituents (20 μM) in 20 mM NaPB (pH 7.4). Solid line, hypericin; dashed line, hyperforin; and dotted line, quercitrin. (B and C) Altered photochemical behavior of SJW-derived photosensitizers by addition of quercitrin (**17**). Photoreactive SJW constituent (20 μM) was exposed to simulated sunlight (250 W/m^2) in the presence of quercitrin at various concentrations, and generation of singlet oxygen (A) and superoxide (B) was monitored. ○, hypericin (**4**); and △, hyperforin (**3**). Data represent mean ± SD of three determinations.

responses. Further investigation on *in vitro* photochemical interaction among quercitrin (**17**) and SJW phototoxins was also carried out using ROS assay (Fig. 5B and C). On the basis of the results from ROS assay on hypericin (**4**) and hyperforin (**3**), they exhibited intense induction of type II photochemical reaction, and type I photochemical reaction was negligible for hyperforin (**3**). Addition of quercitrin (**17**) at various concentrations ranging from 20 to 100 μM resulted in partial changes of ROS generation from the photoirradiated chemicals. There was a ca. 58% reduction of singlet oxygen from hyperforin (**3**), and no significant changes were seen in superoxide. In contrast, only a slight change in photoreactivity of hypericin (**4**) was observed in the presence of quercitrin (**17**), although the latter tended to slightly enhance the type I photochemical reaction of hypericin (**4**). Thus, quercitrin (**17**) tended to modulate the *in vitro* photochemical properties of hyperforin (**3**), the content of which in the SJW extract was calculated to be 3.8%. Considering the low level of hypericin (**4**) (0.12%) in the SJW extract, the modulating *in vitro* photochemical behavior of hyperforin (**3**) might have a major impact on the *in vitro* phototoxic potential of the SJW. The present findings are in agreement with previous observation reported by Wilhelm et al. (2001), and this feature can be a part of the mechanisms behind the protective effect of quercitrin against *in vitro* phototoxicity of the SJW extract. Further investigation on *in vitro* photochemical interaction among major SJW constituents might provide novel insight into the safe use of SJW-based nutraceuticals. In addition, studies on the pharmacokinetic behavior of SJW components might be effective for reliable phototoxic characterization. In particular, the specific distribution of SJW components in skin after oral administration of SJW extract might be of great importance since phototoxic reactions could be mainly caused in the skin.

3. Conclusions

In the present study, the SJW extract and 19 known constituents were characterized with a focus on the *in vitro* photochemical and phototoxicological properties. Exposure of the SJW extract to simulated sunlight resulted in both type I and type II photochemical reactions, and several SJW constituents mimicked the *in vitro* photochemical behavior of SJW extract. Further clarification demonstrated that, of all photoreactive chemicals isolated from the SJW, only hypericin (**4**), pseudohypericin (**5**), and hyperforin (**3**) exhibited photosensitized peroxidation of linoleic acid and no photodynamic cleavage of plasmid DNA, suggesting *in vitro* photoirritant potential. Concomitant UV exposure of hyperforin with quercitrin (**17**), a potent UV/Vis absorber, resulted in the modulated *in vitro* photochemical behavior of hyperforin (**3**). In conclusion, hypericin (**4**), pseudohypericin (**5**), and hyperforin (**17**) might be responsible for the *in vitro* phototoxicity of SJW-based nutraceuticals.

4. Materials and methods

4.1. Chemicals

An *H. perforatum* dry extract 0.3%/ET, a commercially available extract of SJW, I3,II8-biapigenin (**10**), and hyperforin (**3**) dicyclohexylammonium salt were kindly provided by Indena Japan (Tokyo, Japan). Briefly, for preparation of the *H. perforatum* dry extract 0.3%/ET, the flowering tops of SJW were extracted with EtOH–H_2O (7:3 v/v), followed by percolation filtration and concentration. Hyperoside (**12**), I3′,II8-biapigenin (**7**), isoquercitrin (**17**), kaempferol (**14**), luteolin (**15**), and quercitrin (**16**) were purchased from Extrasynthese (Genay, France). Procyanidin B-2 (**11**) was isolated from the leaves of *Eriobotrya japonica* (Ito et al., 2000). GABA (**1**), (−)-epicatechin (**9**), hypericin (**4**), melatonin (**2**), quercetin (**16**), rutin (**18**), butylated hydroxytoluene (BHT), erythromycin, imidazole, linoleic acid, nitroblue tetrazolium (NBT), *p*-nitrosodimethylaniline (RNO), plasmid pBR322 DNA, 1,1,3,3-tetraethoxypropane, TBA, and Tween 20 were obtained from Wako Pure Chemical Industries (Osaka, Japan). (±)-Catechin, mangiferin (**6**), and quinine were purchased from Sigma (St. Louis, MO, USA), and naproxen was obtained from Tokyo Chemical Industry (Tokyo,